Solid-State ^{13}C MAS NMR Studies of Hyper-Cross-Linked Polystyrene Resins

Robert V. Law,† David C. Sherrington,* and Colin E. Snape

Department of Pure and Applied Chemistry, University of Strathclyde, 295 Cathedral Street, Glasgow G1 1XL, U.K.

Isao Ando and Hiromichi Kurosu

Department of Polymer Chemistry, Tokyo Institute of Technology, Ookayama, Meguro-ku, Tokyo 152, Japan

Received October 25, 1995; Revised Manuscript Received May 2, 1996[⊗]

ABSTRACT: ^{13}C CP/MAS NMR techniques have been used to evaluate the structure of four hyper-cross-linked polystyrene resins. Single-pulse excitation (SPE) ^{13}C spectra have allowed the various types of carbon atoms present in the resins to be quantified, and similarly ^{1}H CRAMPS spectra have facilitated quantification of the various hydrogen atom types. Two hyper-cross-linked resins prepared by exhaustive methylene bridging of conventional lightly cross-linked styrene−divinylbenzene resins have very high quaternary aromatic carbon contents. These can be explained adequately only if very high levels of *double* methylene bridging of aromatic groups occurs. Approximately 10% of aromatic groups also retain a chloromethyl group from incomplete methylene bridging. Two further hyper-cross-linked resins reportedly prepared from conventional heavily cross-linked divinylbenzene (55% technical grade) resins appear in one instance to exploit residual unreacted double bonds (and possibly additional divinylbenzene) to generate the secondary cross-links, and in another to use $SOCl_2$/Lewis acid to introduce very high levels of sulfoxide secondary cross-links. Dynamic NMR experiments suggest that the latter two hyper-cross-linked species retain more flexibility and mobility than those prepared via more conventional methylene bridging techniques.

Introduction

Conventional high surface area poly(styrene−divinylbenzene) resin sorbents are generally prepared by using high levels of cross-linker (typically >50 vol %) in the presence of a solvating porogen such as toluene.[1,2] Surface areas of up to ∼600 $m^2\ g^{-1}$ (measured by the N_2 BET method applied to dry beads) are readily achievable. An alternative method of cross-linking polystyrene resin beads is to chemically cross-link preformed linear (or very lightly cross-linked) polystyrene using, e.g., a bishalide and a Lewis acid catalyst. Early materials produced in this way were termed "macronet(work) isoporous" polymers.[3,4] This approach to cross-linking is believed to produce more uniformly cross-linked networks, and bulk physical properties, e.g., swelling, very comparable to those of divinylbenzene cross-linked resins can also be readily achieved in this way.

In the course of the chloromethylation reaction carried out on conventional gel-type and macroporous poly(styrene−divinylbenzene) in synthesizing anion exchange resins, the occurrence of a side reaction involving methylene bridging has been well known for many years.[3,5] Despite this it has proved enormously difficult to produce *quantitative* molecular structural data on the level of methylene bridging, since techniques such as conventional solid-state ^{13}C CP/MAS NMR are not able to count carbon atoms quantitatively.[6] Recently, however, we have made important advances using single-pulse excitation (SPE) ^{13}C solid-state NMR techniques,[7] which can be highly quantitative. Methylene bridging is analogous to the cross-linking reactions used to form "macronet isoporous" polymers. In 1974, Davankov *et al.*[8] introduced what is now generally accepted to be an entirely novel species, the "hyper-cross-linked" network. In these, linear polystyrene in solution is deliberately very heavily cross-linked using similar Friedel−Crafts reactions to those employed to prepare "macronet isoporous" resins. The difference, however, is that it is believed that all pendant aromatic groups become involved in cross-links.[9,10] Spherical beaded analogues of these networks were also produced, based upon lightly (conventionally) cross-linked styrene−divinylbenzene (0.3−2%) resins as the precursor. These materials display some unusual and characteristic physical properties; e.g., the N_2 BET surface areas are typically 800−1000 $m^2\ g^{-1}$, and the materials visibly swell in nonsolvents such as alcohols and even water. To date, it has proved impossible to produce *quantitative* molecular structural data on the true level of cross-linking arising in these materials. However, we have now used SPE ^{13}C solid-state NMR techniques[11] to do just this.

Experimental Section

Materials. Hyper-cross-linked resins H1 and H2 were supplied by Purolite Ltd. These were prepared from two poly(styrene−divinylbenzene) resins, R1 and R2, the first being a gel-type species with a divinylbenzene content of ∼3.5 wt %, the second a macroporous species with a divinylbenzene content of ∼7.5 wt %. R1 and R2 were swollen in a chlorinated solvent, and chloromethyl methyl ether and $SnCl_4$ added. Each mixture was heated at 80 °C for ∼10 h and then cooled to room temperature. The isolated resin was then washed and dried. Procedures were essentially as described by Davankov *et al.*[8,9] Recently, related materials have become commercially available as the Hypersol-Macronet range of sorbents.[12] Hyper-cross-linked resins H3 and H4 were commercially available species supplied by the Mitsubishi Kasei Chemical Corp. as resins Sepabeads SP207 and SP800, respectively. Limited data on these materials have been published.[13] The precursor resin appears to be a poly(styrene−divinylbenzene) species with a divinylbenzene content of ∼55 wt %, and this has been

† Present address: National Institute of Materials and Chemical Research, Higashi 1-1, Tsukubashi, Ibarakiken 305, Japan.

* To whom correspondence should be addressed.

[⊗] Abstract published in *Advance ACS Abstracts,* August 1, 1996.

S0024-9297(95)01606-8 CCC: $12.00

converted to H3 and H4 by procedures similar to these described for H1 and H2 above (see Discussion).

To confirm the presence of residual CH_2Cl groups (see later) on H1, a sample of this was ground to a fine powder mixed with excess of trimethylamine (TMA) in ethanol (25 vol %), and the reaction mixture left at room temperature for 48 h. The resin powder was collected and washed well with water to yield aminated H1, designated H1.AM. Subsequently, a sample of H1.AM was further purified by extraction in a Soxhlet with water, acetone, and, finally, methanol followed by vacuum drying to yield H1.AM.W.

Instrumentation and Analysis. Fourier transform infrared spectra (FTIR) were recorded on a Mattson 5000 FT12 spectrometer. Typically ~250 scans were collected for both the background and the sample. An automatic baseline routine was applied, and spectra were smoothed with a three-point "boxcar" function. The resolution was 4 cm^{-1} and the scanning range 4000−400 cm^{-1}. Samples were prepared as KBr disks, having previously been finely ground using a mortar and pestle. Assignments were made using a standard source.[14]

Elemental microanalytical data were obtained from a Perkin-Elmer Series II 2400 elemental microanalyzer. Though samples were vacuum dried, there was often evidence for trapped water. The oxygen content was calculated by subtracting the total "found" elemental content from 100%. The amount of hydrogen corresponding to this level of oxygen as water was calculated and subtracted from the "found" hydrogen content before computing the C:H ratios. The estimated error for each element analysed was taken as ~±0.5%.

Most of the nuclear magnetic resonance (NMR) spectra were recorded on a Bruker MSL 100 solid-state NMR spectrometer operating at 25.2 MHz for ^{13}C nuclei. The magic angle (MA) was set using KBr. Each ground sample (~200 mg) was packed into a 7 mm o.d. zirconia rotor and sealed with a Kel-F endcap. The samples were spun at ambient temperatures using a Bruker double-bearing probehead. Proton decoupling fields were ~70 kHz. Samples were referenced using either the internal standard, tetrakis(trimethylsilyl)silane (TKS) at 3.5 ppm or the external standard tetramethylsilane (TMS). An exponential line broadening weighting in the range 5−35 Hz was applied to each spectrum.

High-field NMR spectra were recorded on a JEOL GSX 270 NMR spectrometer with a solid-state capability. This operated at ~67.8 MHz for ^{13}C nuclei.

Cross polarization magic angle spinning (CP/MAS) NMR experiments were carried out under the Hartmann−Hahn match condition, which was set using adamantane. The ^1H 90° pulse length was ~3.5 μs, giving a spin-lock and decoupling field strength of ~70 kHz. The experiments were generally carried out with a 1 ms contact time, and a cycle delay of 1.5 s (low-field spectrometer) or 5.0 s (high-field spectrometer). The acquisition time was typically 30 ms, and the spectral width was 30 kHz. Typically 2−8K of points were zero-filled to 16K. Generally 3000−4000 scans were recorded for each sample. Overnight accumulations (30 000+ scans) were carried out for samples of low sensitivity. With the high-field instrument, where spinning sidebands can be a bigger problem, CP/MAS spectra were recorded with total sideband suppression (TOSS), as pioneered by Dixon and co-workers.[15,16] Typically, the acquisition time was 30 ms, spectral width, 27 kHz. 2K of points were zero-filled to 16K, and the proton decoupling field was ~65 kHz. Typical spin rates were 4.0 kHz, and samples were externally referenced to the high-field signal of adamantane (29.5 ppm).

CP/MAS NMR spectra with nonquaternary suppression (NQS)[17] were recorded so that only the nonprotonated and any mobile methyl carbon atoms were visible in the resulting spectra. In order to completely remove the signals from the protonated carbons, a delay of 40 μs was found to be optimum between the contact time and the acquisition time when spinning the sample at 5.0 kHz.

Nuclear Overhauser enhanced (NOE) solid-state NMR spectra were also recorded to enhance the mobile parts of spectra which are often discriminated against using the cross polarization technique. The approach of Findlay and Harris[18] was adopted.

To allow the *quantitative* determination of the amounts of each carbon species in a spectrum, the single-pulse excitation (SPE) method was employed on the low-field instrument.[11,19] In this a time delay of 5 × ^{13}C spin−lattice relaxation time is inserted between pulses. Typically 800−3000 scans were recorded with a delay between each pulse of between 60−100 s. The ^{13}C 90° pulse length was 3.5 μs, and the ^1H decoupling field strength was as before. Typically, acquisition times were between 0.1−0.2 s. To ensure quantitative measurements, tetrakis(trimethylsilyl)silane was used as internal standard for spin counting.[20] This acts as a reference to calibrate the spectra to an accuracy of ±0.3 ppm, but also since its methyl groups have a short ^{13}C T_1 relaxation time, it can be used for "spin counting" in SPE experiments to ensure that the recycle delay is not too short. For quantitative analysis peak areas were determined by cutting and weighing.[11]

Proton spin−lattice relaxation experiments were carried out on a Bruker MSL 100 solid-state NMR spectrometer using the homonuclear wide-line probehead operating at 100.13 MHz for ^1H nuclei. Samples were dried under vacuum at 10^{-6} Torr at 60 °C for 12 h to remove any traces of water. They were then loaded into a 5 mm NMR tube and placed into a horizontal solenoid coil. For a relaxation experiment in the laboratory time frame (T_1), the ^1H 90 pulse length was measured by looking for the null point (the 180° pulse) and then halving this value. The 90° pulse length was typically 3 μs and set using the signal from natural rubber. Spin-lattice relaxation times were determined by two methods with single-point acquisition, namely, inversion−recovery and saturation−recovery. Since the initial point of free induction decay (FID) is proportional to the total intensity of the entire spectrum, it is possible to record only the first point of the FID and plot this as a function of time. Therefore, this technique allows a series of FIDS to be collected as a function of the delay, τ. Typically, 256 or 512 FIDS (single points) are collected with 4 or 8 scans. The inversion−recovery method was used when the sample had a long T_2 and/or a very fast relaxing component. The disadvantage of this technique is that, since it is an equilibrium method, a delay of $5T_1$ is required between each scan. In the saturation−recovery experiment, the system starts a nonequilibrium state with the magnetization in the *xy* plane. The relaxation back to the equilibrium state is monitored as a function of time, τ. The advantage of this sequence is that it is not necessary to wait for a period of $5T_1$ between scans. The decay curve formed by this method was analyzed by a Simplex approximation followed by a Lavenberg−Marquardt approximation.[21] For relaxation experiments in the rotating time frame ($T_{1\rho}$), the single-point acquisition method was used. The proton decoupling field strength was the same as that set up in the CP experiment (~70 kHz) in order to obtain comparable values for the relaxation when determined by this method and CP. The data were analyzed as before.

Proton CRAMPS[22] is a technique that enables "high-resolution" proton spectra to be obtained in the solid state. As in ^{13}C solid-state "high-resolution" NMR spectroscopy, the resolution is usually much less than that in the solution state but it is good enough to resolve the aromatic and aliphatic regions in amorphous polymers. As for solution-state NMR, this technique is quantitative[23−25] and the peak areas are related to the number of protons present in the sample. Even on a commercial spectrometer, this is not a trivial experiment to implement and may account for the dearth of publications compared to solid-state ^{13}C NMR. One of the main features of this technique involves signal acquisition during the pulse sequence and it is very important to minimize many interfering factors, such as phase transient errors and pulse length inequalities.

The spectra were recorded at 100.13 MHz for ^1H using a Bruker CRAMPS probe. The samples were packed into 7 mm o.d. rotors and sealed with a Kel-F rotor endcap. No special precautions were taken against bulk magnetic susceptibility, for example, spherical sample packing, as this is not a problem at low magnetic fields (2.35 T). The magic angle was set using

$KHSO_4$.[23] The ^1H 90° pulse length was set to 1.5 μs, and the probe dead time was 3.0 μs. This was not the initial dead time but was reduced by "spoiling" the Q of the coil circuit by the introduction of several resistors placed in parallel in the rf circuit. The BR-24 multiple pulse sequence[26] was used in preference to the MREV-8[27,28] sequence because it gave better resolution. The problems commonly associated with this sequence were not encountered here.[29] The setting up of the phases, amplitudes, etc. were carried out using the standard flip-flop sequence.[23] Offsets were altered and the spin rate adjusted until the line width was minimized. Typically, 512 points were acquired and zero-filled to 2048 points. A total of 256 scans were accumulated with a delay between each scan of 5 times the proton spin−lattice relaxation time of the sample. The sample spin rate was 2.5 kHz for the BR-24 pulse sequence. As this technique scales the chemical shifts, the samples were run with and without an internal reference and then rescaled accordingly. The internal reference used was either adamantane (1.76 ppm) or TKS (0.2 ppm). This technique gave an accuracy of ±0.5 ppm.[24]

The CRAMPS[30] dipolar (DD) dephasing experiment allows a delay[31] before application of the multiple pulse decoupling sequence. This ensures that the protons that experience strong homonuclear dipole−dipole interaction are selectively dephased. This leaves only the ^1H magnetization due to protons that do not experience strong homonuclear dipolar effects because of the effects of motion averaging. These data were treated qualitatively because of the difficulties in data fitting.

Results and Discussion

Hyper-Cross-Linked Resins H1 and H2. The spectroscopic studies (NMR, FTIR) of these two resins yielded essentially identical data within the experimental limits. Thus, in terms of this molecular structural assessment, there is no discernible difference between starting with a precursor resin which is a gel type (R1 → H1) and one which is macroporous (R2 → H2). Differences in porosity, and in particular the balance between micro-, meso-, and macropores, would of course be anticipated but this does not fall within the scope of the present investigation. Bearing this in mind, detailed results will be presented for H1 only.

Elemental Microanalytical and FTIR Studies. The elemental microanalytical data for H1 are as follows: C, 82.7%; H, 5.8%; Cl, 3.8%; O, 7.7%. The last figure was arrived at by difference, and this oxygen content seems to arise primarily from the trapped water but also includes oxygen in hydroxymethyl groups (see later). There is no detectable nitrogen content. Using the method described in the Experimental Section, the atomic ratio of C:H was calculated as 1.43:1.00 and of C:Cl as 9.78:1.00. The theoretical C:H ratio for linear polystyrene is 1:1 and for the idealized methylene-bridged structure (**1**), (Figure 1) it is 1.06. The very high value obtained experimentally cannot therefore be rationalized simply in terms of methylene bridging (or indeed multiple bridging). Almost certainly this is an artifact arising from the attempt to account for the oxygen as water, which necessarily requires deletion of significant hydrogen.

The most important feature of the analytical data however is the significant chlorine content. This arises from residual unreacted chloromethyl groups (**2**) (Figure 1) but may also have a contribution from trapped catalyst or its residues. The level of the latter is low however since no significant inorganic residue was recorded in the combustion analysis. An order of magnitude calculation shows that substitution of ~10% of aromatic groups with CH_2Cl is required to account (alone) for this chlorine content.

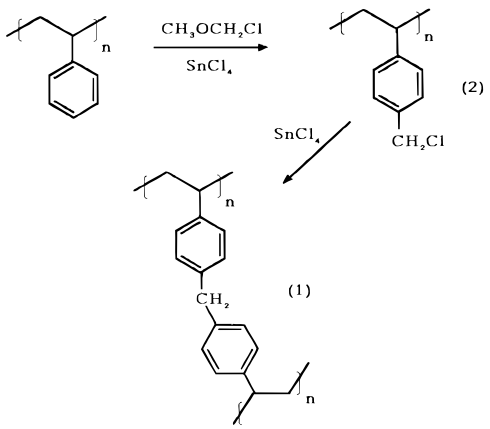

Figure 1. Chloromethylation of polystyrene resins showing formation of methylene bridges (secondary cross-links).

Table 1. Assignment of FTIR Bands for H1

structural group	wavenumber (cm^{-1})
OH and water	3425
aromatic C−H str	3078, 3045, 3014
aliphatic C−H str	2920, 2856, 2733
overtones/ combinations C−H def	1905, 1847
C═O str	1699, 1678
C═C str	1633, 1606, 1510, 1440, 1018
CH_2Cl wag	1265
C−O−C str (?)	1110
aromatic ring def	816, 704
C−Cl str	748, 679, 607

The assignment of the FTIR absorption bands is shown in Table 1. The most intense of these (below 2000 cm^{-1}) is at 816 cm^{-1}, which together with the aromatic C═C stretch peak at 1510 cm^{-1} is attributed to para-substituted aromatic rings. This would correspond to the methylene bridge structures (**1**) (Figure 1). The spectrum here is slightly different from those described previously by Davankov *et al.*,[9] who reported a peak at 820 cm^{-1} corresponding to para substituted aromatic rings, but also a peak at 756 cm^{-1}. The latter usually corresponds to a monosubstituted benzene ring, such as those in polystyrene. In the resin (H1) analyzed in the present work no such peak was found, implying that all the benzene rings are at least disubstituted. Another feature of the spectrum is the presence of the carbonyl peaks at 1699 and 1678 cm^{-1}. This finding is confirmed later in the ^{13}C NMR spectra. The frequency of these is indicative of the presence of either a carboxylic acid or an ester and is discussed later. Other features of the spectrum are the peaks at 1633 and 1018 cm^{-1} indicative of vinyl groups. These may arise from a small level of unreacted double bonds from the original divinylbenzene cross-linker used to prepare precursor resin R1, or through a cleavage reaction proposed previously[13] (Figure 2).

The presence of chloromethyl, CH_2Cl, groups is confirmed by the $-CH_2-$ wag peak at 1265 cm^{-1} associated with which is the signal at 679 cm^{-1} assigned to the C−Cl stretch. The assignment of the peak at 1110 cm^{-1} is uncertain. It could arise from an ether linkage but these are generally difficult to specify by IR spectroscopy alone because there are many other peaks that arise from styryl residues in this region.

Low-Field (25.2 MHz) 13C NMR Studies. The low-field ^{13}C CP/MAS NMR spectrum of H1 is shown in Figure 3 (bottom) along with the corresponding NQS spectrum (top). The main assignments are also indi-

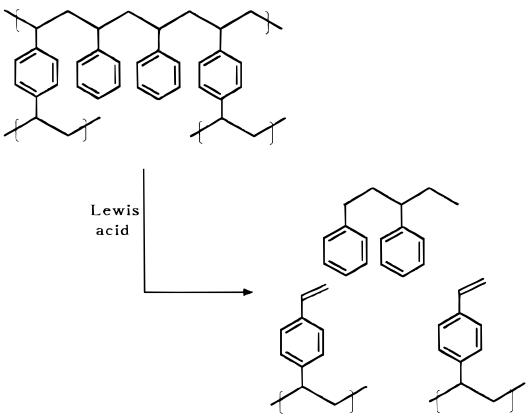

Figure 2. Possible degradative cleavage reactions of polystyrene resins catalyzed by Lewis acids.

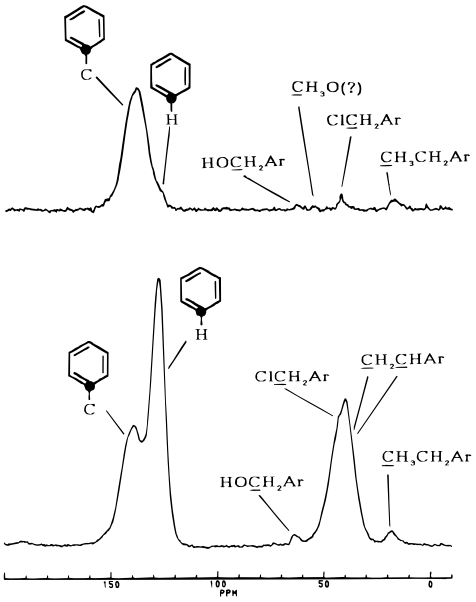

Figure 3. Solid-state (25.2 MHz) ^{13}C NMR spectra of H1: (top) NQS spectrum, ns = 4656; (bottom) CP spectrum, ns = 5664, RD = 1.5 s, LB = 10 Hz (ns = number of scans; RD = recycle delay time; LB = exponential line broadening weighting).

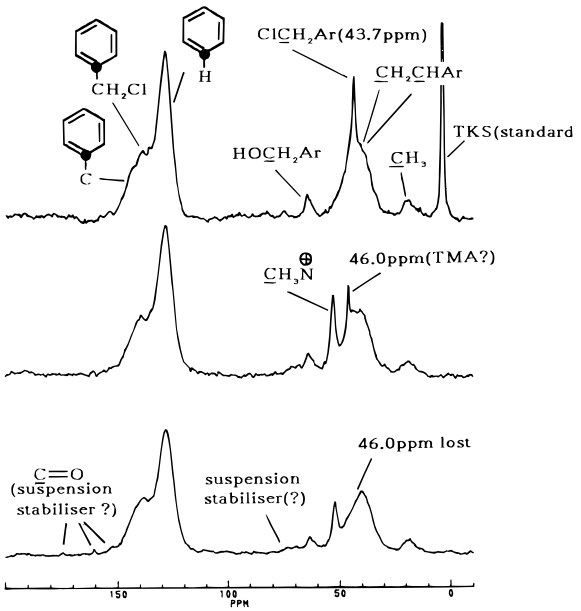

Figure 4. Solid-state (25.2 MHz) ^{13}C NOE NMR spectra of: (top) H1, ns = 3210, pulse train = 5 s; (middle) H1.AM, ns = 4188, pulse train = 5 s; and (bottom) H1.AM. W, ns = 2621, pulse train = 15 s, LB = 15 Hz (for ns, RD, and LB, see Figure 3 caption).

cated and are similar to those of the lightly cross-linked precursor resin, R1.[7] The presence of the quaternary aromatic carbons, protonated aromatic carbons, and the aliphatic main-chain methylene and methine carbons is clear. There are several other interesting features however. There is a peak at 64.8 ppm which is characteristic of a hydroxymethyl carbon. This group might arise from hydrolysis of pendant chloromethyl moieties during synthesis as suggested previously.[32,33] There is also a small shoulder on the methylene–methine peak at 43.6 ppm. This is assigned to the chloromethyl carbon, and more evidence will be provided to support this shortly. Finally, the peak at 19.3 ppm is attributed to a methyl carbon present in the precursor resin, R1. This has its origins in the ethylstyrene contaminant of technical divinylbenzene. The signal from the associated methylene carbon atom is probably contained within the broad resonance centered ~40 ppm, although it is resolved in the spectra of H3 and H4, which have much higher levels of such ethyl groups (see later and Figure 14). It is interesting to note that both the chloromethyl and methyl carbon peaks have chemical shifts slightly different from those we have reported for the chloromethylated intermediate in the synthesis of conventional anion exchange resins.[7] This will be rationalized shortly.

In the NQS spectrum the asymmetrical shape of the quaternary aromatic carbon peak is most likely due to the methylene bridge substituents. The aliphatic carbon region is particularly interesting with residual peaks at 64.8 and 43.6 ppm confirming the presence of mobile hydroxymethyl and chloromethyl carbons. There is also a small peak at 57.1 ppm which may possibly be due to a methoxy carbon but it is too small in intensity to be certain. The mobile methyl group identified above can also be seen at 19.3 ppm.

The NOE spectrum of H1 (Figure 4 (top)) is as expected and the major peaks are the same as before. Additional low-intensity signals appear in the carbonyl region (seen more clearly in Figure 4 (bottom)) and these correlate nicely with the carbonyl absorptions seen in the FTIR spectrum (Table 1). The origin of these carbonyl functions is difficult to confirm but they may be associated with trapped polymerization suspension stabilizer, as could be the mobile carbon atom responsible for the small peak at 74.8 ppm, the associated aliphatic carbon signals being contained within the broad envelope ~40 ppm. The quaternary carbon signal (Figure 4) shows two peaks at 139.2 and 136.4 ppm. The former appears to be due to the usual carbon attached to the polymer backbone. The latter is tentatively assigned to those carbon atoms bound to a chloromethyl carbon. The small difference in the chemical shift here compared to that we reported earlier[7] is likely to be due to differences in the proportions of disubstituted and trisubstituted aromatic rings (see later). The hydroxymethyl peak can be seen clearly at 64.8 ppm and is much more intense than in the CP/MAS spectrum, again due to the high mobility of this group. The methyl peak seen earlier at 19.3 ppm is here comprised of many resonances from 20 to 13 ppm, while the peak at 3.5 ppm is from the internal standard TKS.

In the case of the carbon atoms in the chloromethyl and methyl groups, there are slight changes in the chemical shifts from those previously found in chloro-

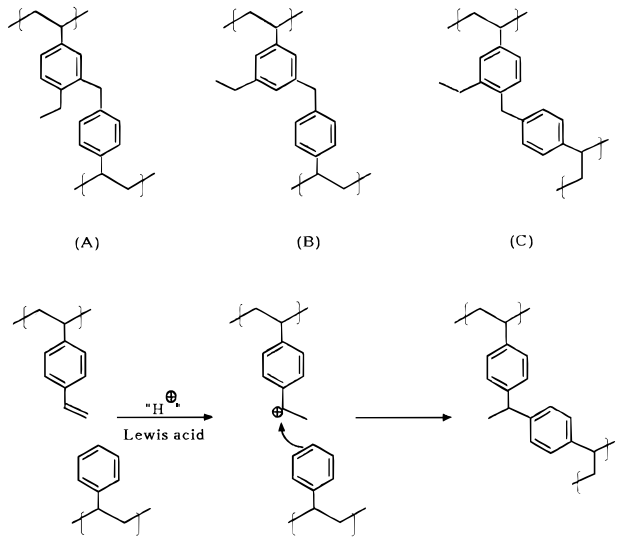

Figure 5. Possible configurations of methylene bridges and ethyl substituents in secondary cross-linked poly(styrene−divinylbenzene) resins (A, B, C), and possible mechanism for secondary cross-linking involving unreacted double bonds and Lewis acid in poly(styrene−divinylbenzene) resins.

methylated resins.[7] Again the reason for this may be the difference in the proportions of di- and trisubstituted aromatic rings. In the case of the chloromethyl carbon, the earlier value[7] was 46.8 ppm compared with 43.7 ppm in the present resins. This may seem a rather big difference but the methylene carbon resonance in *p*-(chloromethyl)toluene is at 46.1 ppm, and that in (chloromethyl)-p-xylene at 44.9 ppm. This confirms that shifts of this size are not at all unusual, and indeed should be anticipated. The presence of trisubstituted aromatic rings may also account for the distribution of chemical shifts that arise for the methyl groups. Those groups which originate in the ethylstyrene residues (the technical divinylbenzene contaminant) in the precursor copolymer, R1, may also be influenced by methylene bridging in various ways (Figure 5) though the initial lightly cross-linked nature of R1 demands that the proportion of these structures is low. The increase in intensity of the methyl peak relative to that in the precursor R1 and the absence of a discrete signal from the methylene group of the ethyl substituent at ∼29 ppm suggest that there is another source of methyl groups in the resin. These may arise, for example, from an additional cross-linking process proposed earlier[13] involving reaction of residual unreacted double bonds (Figure 5).

High-Field (67.8 MHz) 13C NMR Studies. The ^{13}C CP/MAS NMR spectrum of H1 showing the effect of increasing the field strength on the sample appears in Figure 6. This is similar to that obtained at low-field however, the resolution is slightly enhanced. The quaternary aromatic carbon peak at 139.2 ppm is made of approximately four resonances. The hydroxymethyl peak is present at 69 ppm but this is slightly obscured by the presence of a broad spinning sideband superimposed upon it. The methylene−methine peak at 40.9 ppm is now accompanied by a small peak at 43.7 ppm which is attributed to the chloromethyl carbon. This is more evident than at low-field. The methyl peak at 19.3 ppm is made up of several resonances, similar to those observed at low-field. However, because a second-order spinning sideband lies at the same position, the intensity of the methyl group is distorted. Also present is a carbonyl group at 154 ppm. The peak at 166 ppm is

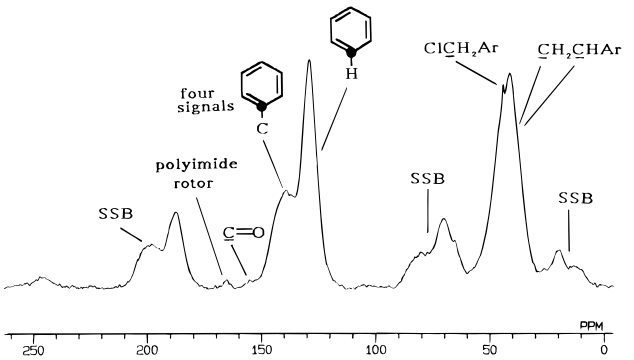

Figure 6. High-field solid-state (67.8 MHz) ^{13}C CP/MAS NMR spectrum of H1, ns = 2341, RD = 5 s, LB = 5Hz (for ns, RD, and LB, see Figure 3 caption).

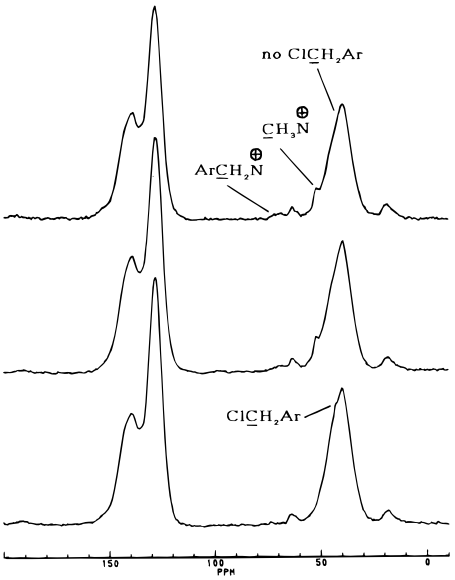

Figure 7. Solid-state (25.2 MHz) ^{13}C CP/MAS NMR spectra of: (top) H1, ns = 3504; (middle) H1.AM, ns = 5088; (bottom) H1.AM.W, ns = 5664, LB = 10 Hz (for ns, RD, and LB, see Figure 3 caption).

due to the polyimide rotor cap and may mask other carbonyl peaks. Overall, however, the high-field spectrum confirms the interpretations placed on the low-field data.

Amination of Resin H1. Resin H1 was treated with TMA in order to try to substantiate two hypotheses: first, that the peak at 43.7 ppm is in fact due to the chloromethyl group carbon and second, to confirm that these groups are available for further reaction, contrary to an earlier statement in the literature.[34] The low-field ^{13}C CP/MAS[34] spectra for resin H1 (bottom), H1.AM (middle), and H1.AM.W (top) are shown in Figure 7. The spectra are essentially identical in the aromatic region, or at least the shifts which do occur are not apparent and are accommodated under the broad aromatic envelope. New peaks do occur, however, at 69.0 and 53.0 ppm. They are accounted for by the formation of quaternary ammonium groups similar to those formed when conventional chloromethylated polystyrene resins are treated with a tertiary amine in the synthesis of anion exchange resins.[7] The peak at ∼69 ppm appears as a small broad shoulder and can be assigned to the CH_2N^+ carbon, and the sharper signal at 53.0 ppm on the side of the methylene−methine peak can be attributed to the CH_3N^+ carbon. Very importantly, the peak corresponding to the chloromethyl carbon has

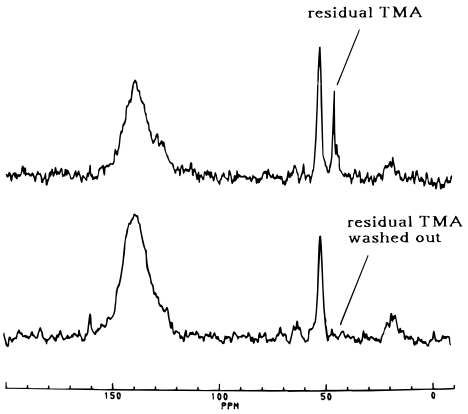

Figure 8. Solid-state (25.2 MHz) ^{13}C NMR NOENQS spectra of (top) H1.AM, ns = 3461; (bottom) H1.AM.W, ns = 2621, pulse train = 15 s, LB = 15 Hz (for ns, RD, and LB, see Figure 3 caption).

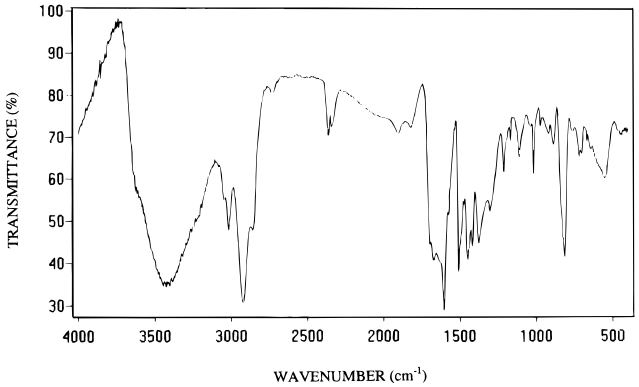

Figure 9. FTIR spectrum of resin H1.AM.W.

disappeared. The NQS spectrum (not reproduced here) confirms this picture.

The NOE spectrum of H1.AM (Figure 4 (middle)) is more revealing than its CP/MAS counterpart. The sharp signal from the carbon in the mobile CH_3N^+ group is now very evident at 53.1 ppm and is accompanied by a new sharp resonance of 46.0 ppm (Figure 4 (top)). Initially, it was thought that this might be due to unreacted chloromethyl groups; however, the chemical shift is too high compared to that seen earlier in H1 (43.7 ppm). This feature therefore seems to be associated with trapped TMA. To check this assignment, the resin was exhaustively extracted to yield the "clean" species, H1.AM.W. This indeed yields a spectrum in which the 46.0 ppm resonance is absent (Figure 4 (bottom)). The loss of this peak is confirmed most unambiguously in NOENQS spectra of HA1.AM and H1.AM.W (Figure 8). This result provides a cautionary lesson therefore that with these very highly cross-linked resin systems care is required in washing and purification steps to remove residual non-chemically bound contaminants.

The successful amination of the residual chloromethyl groups in H1 is confirmed by the FTIR spectrum of H1.AM.W (Figure 9). The important absorption bands which have disappeared are the chloromethyl wag at 1265 cm^{-1}, and the corresponding stretching bands at 748, 679, and 607 cm^{-1}. These are replaced by absorptions at 1379, 766, and 721 cm^{-1} arising from the $CH_2N^+(CH_3)_3$ group. The elemental microanalytical data for H1.AM.W also confirm the incorporation of nitrogen (C, 75.1%; H, 6.7%; Cl, 0.7(6)%; N, 0.4(5)%). Though the absolute values of Cl and N are low and

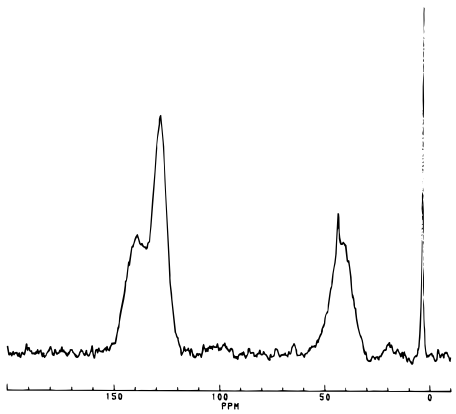

Figure 10. Solid-state (25.2 MHz) ^{13}C SPE NMR spectrum of H1, ns = 1250, LB = 10 Hz, RD = 60 s (for ns, RD, and LB, see Figure 3 caption).

Table 2. Ratio of Peak Areas in SPE Spectrum of H1

carbon atom types	atomic ratios exptl	atomic ratios theor[a]
Ar_{total}:Al_{total}	2.05:1.00[b]	2.40:1.00
protonated Ar:quaternary Ar	1.70:1.00[c]	2.00:1.00
Ar_{total}:chloromethyl	~100:1.00	
Ar_{total}:methyl	~55:1.00	
Ar_{total}:carbonyl	>100:1.00	

[a] Based on structure **1** (Figure 1). [b] Error ±10%. [c] Error ±20% (signal overlap).

therefore subject to a large percent error, the ratio of Cl/N is reasonably close to the 1/1 molar ratio expected for $CH_2{}^+N(CH_3)_3Cl^-$ groups.

Quantitative Structural Analysis of H1. The single-pulse excitation (SPE) ^{13}C NMR spectrum of H1 is shown in Figure 10. The ratios of the peak areas here *can* be used to quantify the various types of carbon atom present in the resin,[7,11] from which the level of methylene bridging can be deduced. The theoretical ratio of total aromatic carbons to total aliphatic carbons, Ar_{tot}:Al_{tot}, based on the model methylene-bridged structure (**1**) (Figure 1) is 2.40:1.00 (Table 2). The experimentally determined value is 2.05:1.00. This confirms the very heavy level of methylene bridging, but since the ratio is even less than predicted from structure **1**, it suggests that additional aliphatic carbon functionality arises, yielding trialkyl-substituted aromatic rings. The low ratio of protonated aromatic carbons to quaternary aromatic carbons (found: 1.70:1.00; for structure **1** (Figure 1) 2.00:1.00) tends to confirm this. The elemental microanalytical data earlier suggested ~10% of aromatic groups might carry a chloromethyl moiety, and the ratio of total aromatic carbon to chloromethyl carbon found in the SPE spectrum (Table 2) is not inconsistent with this picture. The high aliphatic carbon content therefore is accounted for in part by structures such as **3** (Figure 11). However, ~10% of aromatic groups involved in such structures would not alone account for the observed Ar_{tot}:Al_{tot} ratio of 2.05:1.00. To achieve this requires, for example, nearly all aromatic rings each to be linked by *two* methylene groups. The dihydroanthracene structure, **4**, (Figure 11), conforms to this picture and has been proposed before.[35] A perfectly plausible mechanism is available for formation of this, but such a structure would require the bridging carbon atoms to appear as a resonance at ~33 ppm in the ^{13}C NMR spectrum and this is not the case experimentally. The required double methylene bridges must therefore arise from an appropriate statistical distribution of

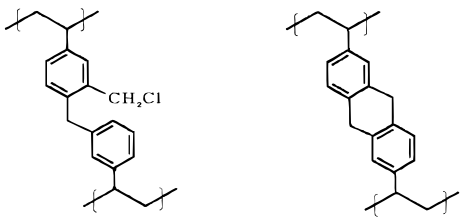

(3) (4)

Figure 11. Additional methylene bridge structures arising as secondary cross-links in chloromethylated polystyrene resins.

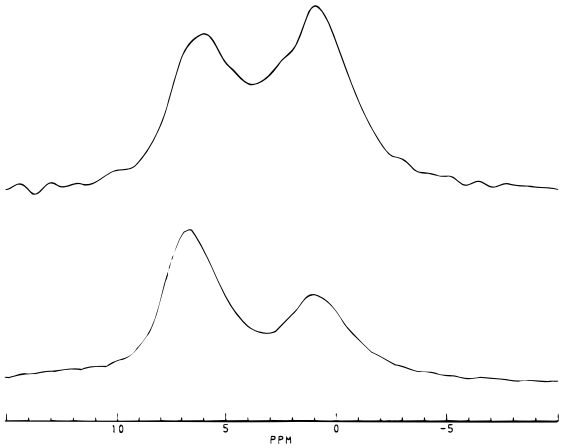

Figure 12. Solid-state (100.13 MHz) ^{1}H CRAMPS NMR spectra of: (top) H1, ns = 512; (bottom) R1, ns = 512; RD = 30 s, no line broadening (for ns, RD, and LB, see Figure 3 caption).

Table 3. Aromatic:Aliphatic Proton Ratios from ^{1}H CRAMPS Spectra of R1 and H1

	Ar:Al proton ratios	
resin	exptl[a]	theor
R1	1.52:1.00	1.67:1.00[b]
H1	0.81:1.00	1.00:1.00[c]

[a] Error ±10%. [b] Linear polystyrene model. [c] Based on structure **1** (Figure 1).

methylene bridges between all aromatic groups. Providing sterechemical limitations do not arise, the occurrence of double methylene bridging is of course consistent with activation of the aromatic rings following alkylation in the initial methylene bridging.

The ^{1}H CRAMPS spectra of H1 and its precursor resin R1 are shown in Figure 12 and display resolution similar to that of a solid-state ^{13}C spectrum. The technique is again quantitative for counting proton types in this case.[23−25,30] The experimental ratios of aromatic:aliphatic protons for H1 and R1 are shown in Table 3. For R1 this ratio is a little lower than that for linear polystyrene and the deviation is reasonable, based on the presence of small amounts of divinylbenzene and ethylstyrene residues present in R1, the aromatic:aliphatic proton ratios being 0.67:1.00 and 0.50:1.00, respectively, for these. The spectrum of H1 is similar to that of R1 but with crucial differences in peak shapes and intensities. The aromatic signal appears to be comprised of two broad reasonances and may be indicative of high para substitution of rings. There is also a small shoulder at ∼3 ppm on the aliphatic peak indicative of a different proton on an aliphatic carbon, or possibly due to H_2O. The shifts in peak shapes and intensities clearly arise from groups

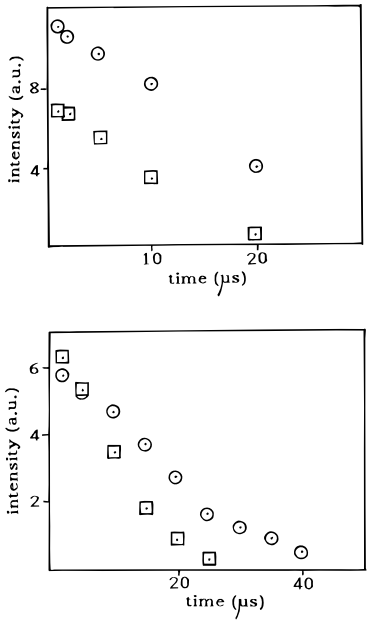

Figure 13. Intensity−time plots for the ^{1}H CRAMPS dipolar dephasing (DD) experiments: (top) R1; (bottom) H1. In each case, (⊙) = aromatic protons and (⊡) = aliphatic protons (a.u. = arbitrary units).

Table 4. Proton Relaxation Data[a] for Resins

resin	T_1 (s)	$T_{1\rho}$ (ms)
R1	1.55	60
H1	1.33	35
H3	1.92	73
H4	3.70	186

[a] Error ±5%.

introduced during secondary cross-linking, but the exact nature of the protons cannot be determined. The ratio of aromatic:aliphatic protons changes very significantly to 0.81:1.00 (Table 3). The ratio for the idealized methylene-bridged structure (**1**) (Figure 1) is 1.00:1.00 and so clearly in practice the proportion of aliphatic protons is increased far beyond this. While chloromethyl protons make a contribution, a ratio of 0.81:1.00 can be realized only if the level of double methylene bridging (or its equivalent) is very high. Structure **4** (Figure 11) and the more likely randomized double bridging structures corresponding to this yield an aromatic:aliphatic proton ratio and 0.6:1.00. Hence the ^{1}H CRAMPS spectra confirm the ^{13}C SPE data that very high levels of double methylene bridging arises in H1.

Dynamic ^{1}H NMR Data. The intensities of the dipolar dephasing spectra[36] of R1 and H1 are plotted against time in Figure 13. For R1 the gradients of the signals from the aromatic protons and from the aliphatic protons are the same. This reflects a uniform degree of proton homonuclear interaction in the sample. With H1, however, the aliphatic signal dephases much faster than the aromatic one and is accounted for by the greater rigidity of the aliphatic protons in the methylene bridges which consequently experience a stronger homonuclear interaction.

Data from the ^{1}H broad line relaxation experiments are shown in Table 4. When R1 undergoes additional cross-linking to form H1 both T_1 and $T_{1\rho}$ are shortened. Again this is clear indication of cross-linking. It is interesting to note, however, that although $T_{1\rho}$ is shorter for H1, it is still longer than that for a resin prepared from 100% *p*-divinylbenzene.[37] This suggests that the

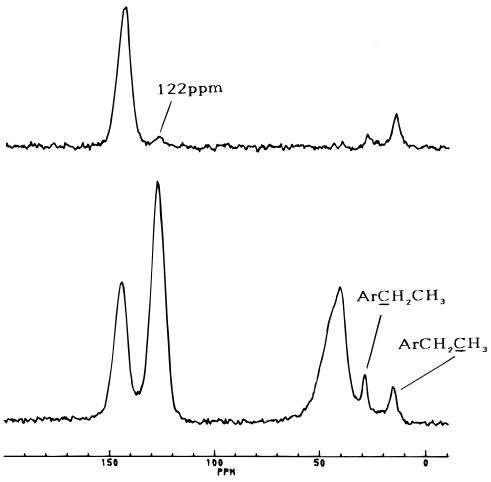

Figure 14. Solid-state (25.2 MHz) ^{13}C NMR spectra of H4: (top) NQS spectrum, ns = 4000; (bottom) CP spectrum, ns = 4000; RD = 1.5 s, LB = 10 Hz (for ns, RD, and LB, see Figure 3 caption).

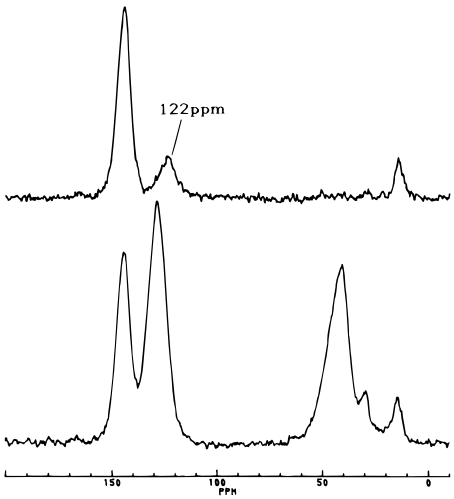

Figure 15. Solid-state (25.2 MHz) ^{13}C NMR spectra of H3: (top) NQS spectrum, ns = 4000; bottom, CP spectrum, ns = 4000; RD = 1.5 s, LB = 10 Hz (for ns, RD, and LB, see Figure 3 caption).

latter is even more tightly cross-linked than H1 and certainly that the structures involved are quite different. It might be, for example, that H1 has a higher degree of order within the very tight network and that the ~100% DVB resin has more entanglements. The swelling behavior of 100% divinylbenzene resins has been reported[38] to be quite different from that of 88 and 55% divinylbenzene/styrene analogues, and indeed there is some similarity between the bulk properties of the 100% divinylbenzene resins and those of hyper-cross-linked species.

Structural Analysis of Resins H3 and H4. The ^{13}C CP/MAS and NQS NMR spectra of H4 are shown in Figure 14. These differ from the corresponding spectrum for H1 (Figure 3) in the clearer resolution of the two aromatic signals and the stronger methyl carbon signal at ~18.0 ppm. There is also a sharp resonance at ~30 ppm, which we assign to the methylene carbon in ethyl groups derived from the ethylstyrene in commercial DVB. The latter is much suppressed in the NQS spectra. H4 is reported to be prepared from a ~55% cross-linked precursor resin,[13] and if so will indeed contain substantial levels of ethyl groups from the ethylstyrene contaminant of divinylbenzene. The strong methyl carbon signal at ~18.0 ppm confirms this. The methyl group would be expected to be very mobile and the signal is indeed retained in the NQS spectrum. Secondary cross-linking of H4 using a Lewis acid and exploiting the existing residual double bonds (from incomplete reaction of divinylbenzene in forming the precursor resin) would generate the additional cross-link structures shown in Figure 5. (Note: Additional divinylbenzene monomer may also be introducing during this secondary reaction.) An additional major difference between the spectra of H1 (Figure 3) and those of H3 (Figure 15) is the appearance of the substantial signal at 122 ppm in the NQS spectrum of H3. (Note: this also appears at lower intensity in the NQS spectrum of H4 (Figure 14).) This feature has proved very difficult to assign. It is tempting to suggest it arises from the methylene carbon in unreacted vinyl groups, but the chemical shift is not correct, and signals from such groups would disappear in the NQS spectrum. It would also be convenient if the chemical shift of an aromatic carbon attached to a sulfoxide group was ~120 ppm, since as indicated below, H3 contains substantial levels of such groups. However, this is not the case and

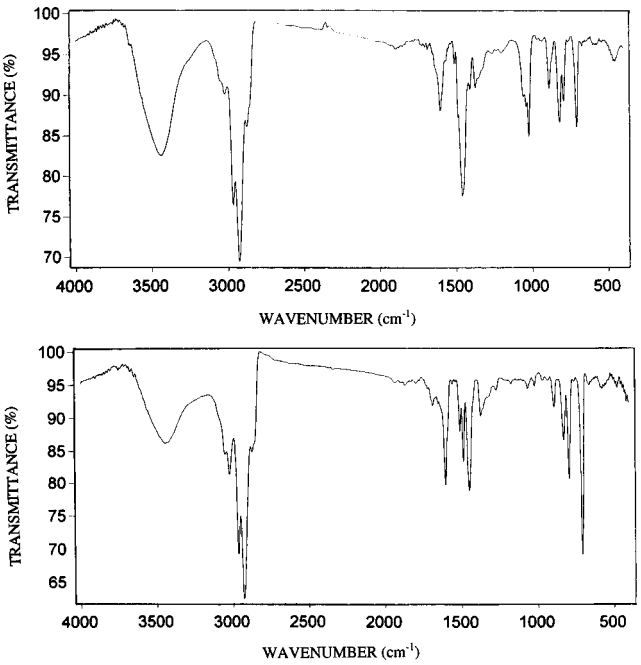

Figure 16. FTIR spectra of H3 (top) and H4 (bottom).

such resonances appear at ~140−145 ppm. The signal at 122 ppm may therefore simply be a residual protonated aromatic resonance in the NQS spectrum, but this is by no means clear.

The FTIR spectra of H3 and H4 are shown in Figure 16. Absorption bands at ~1510 and 825 cm^{-1} in each spectrum confirm the presence of para-substituted aromatic groups, and at 793 cm^{-1} the presence of meta ones as well (again this correlates with the high meta and para contents of technical grade divinylbenzene). There is however a major difference in that the H3 spectrum has intense bands at 1055 and 1022 cm^{-1} characteristic of the S=O group. In the FTIR spectrum of H4, the C=C stretch region is also much better resolved, and the loss of resolution in H3 may be due to the presence of the S=O substituent.

Confirmation for the sulfone presence is afforded by the elemental microanalytical data (Table 5). H3 is found to contain ~16% S and a substantial level of chlorine. The S, Cl, and indeed the O levels of H4 are much lower. Indeed, from this point of view, H4 seems

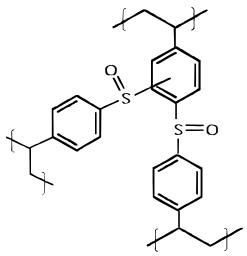

Figure 17. Proposed sulfone bridge, secondary cross-link in resin H3.

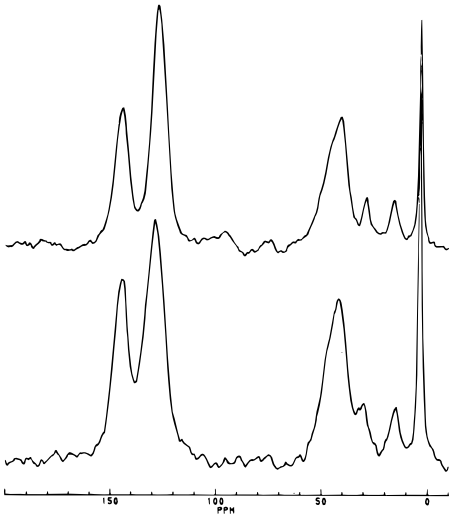

Figure 18. Solid-state (25.2 MHz) ^{13}C SPE NMR spectra of (top) H4, ns = 2488; and (bottom) H3, ns = 2514; RD = 60 s, LB = 35 Hz (for ns, RD, and LB, see Figure 3 caption).

Table 5. Elemental Microanalytical Data and Atomic Ratios for H3 and H4

	elemental microanalytical data (%)				
resin	C	H	Cl	S	O
H3	58.7	4.7	8.7	16.1	11.8
H4	90.1	8.1	0.5	0.7	0.6

	atomic ratios			
resin	C:H	C:S	C:Cl	S:Cl
H3	1.16:1.00	9.78:1.00	19.8:1.00	2.02:1.00
H4	0.94:1.00	348:1.00	532:1.00	1.53:1.00

to be the cleanest resin of all those studied. The ratio of sulfur to oxygen in H3 is such that sulfone groups (SO_2) are unlikely and the most probable secondary cross-linking structure in this resin is the sulfoxide bridge shown in Figure 17. This could readily arise if secondary cross-linking was performed with $SOCl_2$ and a Lewis acid, and might also account for the Cl level of 8.7% in H3, arising from trapped SOCl groups and from Lewis acid fragments. The aromatic ratios calculated from the elemental microanalytical data are also shown in Table 5. The value of 9.78:1.00 for C:S implies that there may be as many as one S atom per aromatic ring. If all S=O groups are also associated with cross-links, this requires many aromatic groups to be bridged by more than one sulfone linkage (Figure 17). In both H3 and H4 the C:H ratios are reasonably close to 1.00:1.00, the theoretical figure for linear polystyrene. This ratio is also consistent with various cross-linking structures proposed for H3 and H4.

The ^{13}C SPE NMR spectra of H3 and H4 are shown in Figure 18. Once again, the spectra allow quantification of the types of carbon atoms present in the resins,

Table 6. Carbon Atom Ratios from ^{13}C SPE NMR Spectra for H3 and H4

resin	Ar_{tot}:Al_{tot}[b]	protonated Ar:quaternary Ar[c]	Ar_{tot}:MM[a,c]	Ar_{tot}:methyl[c]
H3	1.65:1.00	1.71:1.00	2.13:1.00	13.0:1.00
H4	1.60:1.00	1.69:1.00	1.35:1.00	13.5:1.00

[a] MM = methylene−methine backbone carbons. [b] Error ±10%. [c] Error ±5%.

and the data calculated are shown in Table 6. Comparison with the same data for H1 (Table 2) shows that for both H3 and H4 the total aromatic:total aliphatic carbon, Ar_{tot}:Al_{tot}, is much less, ~1.6:1.0 versus ~2.0:1.0 for H1. This is consistent with the high levels of ethyl groups present in H3 and H4 arising from the original ethylstyrene content of the precursor resins.[13]

The ratio of total aromatic to methyl carbons, Ar_{tot}:methyl, in H3 and H4 is also quite different from that in H1, the proportion of methyl groups being more than 4 times higher in the former resins. If it is assumed that H3 and H4 originate only from divinylbenzene and ethylstyrene residues (and no other methyl groups are generated during secondary cross-links), the data suggest that H3 originates from a comonomer mixture of 46% ethylstyrene and 54% divinylbenzene and H4 from 44% ethylstyrene and 56% divinylbenzene. Both data are very close to the typical compositions of technical grade divinylbenzene!

The ^1H spin−lattice relaxation times for H3 and H4 are shown in Table 4. These data are similar to those obtained for polystyrene and in each case the times are longer than for H1 and indeed for R1, the lightly cross-linked precursor to H1. Direct comparison of the data must be made cautiously however. What is clear, however, is that H4 is effectively "less cross-linked" than H3 or, perhaps more realistically, is a more mobile matrix and that both H3 and H4 have higher mobility than H1. This suggests that using a lightly cross-linked precursor resin followed by exhaustive methylene bridging does result in a tighter less mobile matrix than those produced by secondary reactions on a more heavily (conventionally) cross-linked precursor polymer. Since the details of the post-treatments used in H3 and H4 are not available from the manufacturers, further analysis does not seem justified.

Acknowledgment. We acknowledge the receipt of a CASE studentship for R.V.L. from the then SERC and the additional support of the Purolite Co. We are also grateful to the Mitsubishi Kasei Chemical Corp. for the gift of resins and to The British Council and the Tokyo Institute of Technology for their support in enabling R.V.L. to conduct the high-field NMR work in Japan.

References and Notes

(1) Albright, R. L. *Reactive Polym.* **1986**, *4*, 155.
(2) Guyot, A. In *Syntheses and Separations Using Functional Polymer*; Sherrington, D. C., Hodge, P., Eds.; J. Wiley and Sons: Chichester, UK, 1988; Chapter 1, p 1.
(3) Anderson, R. E. *Ind. Eng. Chem. Prod. Res. Dev.* **1964**, *3*, 85.
(4) Samsonov, G. V. ; Trostyanskaya, E. B.; El'kin, G. E. *Ion Exchange Sorption of Organic Substances*, Chimia: Leningrad, 1969.
(5) Pepper, K. W.; Paisley, H. M.; Young, M. A. *J. Chem. Soc.* **1953**, 4097.
(6) Belfer, S.; Glozman, R.; Deshe, A.; Warshawsky, A. *J. Appl. Polym. Sci.* **1980**, *25*, 2241.
(7) Law, R. V.; Sherrington, D. C.; Snape, C. E.; Ando, I.; Korosu, H. *Ind. Eng. Chem. Res.* **1995**, *34*, 2740.
(8) Davankov, V.; Tsyurupa, M. P.; Rogozhin, S. V. *J. Polym. Sci., Polym. Symp.* **1974**, *47*, 95.

(9) Davankov, V. A.; Tsyrurupa, M. P. *React. Polym.* **1990**, *13*, 27.
(10) Rosenberg, G. I.; Shabawa, A. S.; Moryakov, V. S.; Musin, T. G.; Tsyurupa, M. P.; Davankov, V. A. *React. Polym.* **1983**, *1*, 175.
(11) Snape, C. E.; Axelson, D. E.; Botto, R. E.; Delpuech, J. J.; Tekely, P.; Gerstein, B. C.; Pruski, M.; Maciel, G. E.; Wilson, M. A. *Fuel* **1989**, *68*, 547.
(12) Dale,J. A.; Nikitin, N. V. Technical Notes on Hypersol-Macronet, Purolite Int., S. Wales, UK.
(13) Ando, K.; Ito, T.; Teshima, H.; Kusano, H. Proceedings of SCI Symposium IEX 88, Cambridge, UK, 1988 (published in *Ion Exchange for Industry*, Streat, M., Ed.; Ellis Horwood Ltd.: Chichester, UK, 1988; p 232).
(14) Lin-Vien, D.; Colthup, N. B.; Fately, W. G.; Grasselli, L. G. *The Handbook of Infra-Red and Raman Characteristic Frequencies of Organic Molecules*; Academic Press: London, 1991.
(15) Dixon, W. T.; Schaefer, J.; Sefcik, M. D.; Stejskal, E. O.; McKay, R. A. *J. Magn. Reson.* **1982**, *49*, 341.
(16) Dixon, W. T. *J. Chem. Phys.* **1982**, *77*, 1800.
(17) Alemany, L. B. ; Grant, D. M.; Alger, T. G.; Pugmire, R. J. *J. Am. Chem. Soc.* **1983**, *105*, 6697.
(18) Findlay, A.; Harris, R. K. *Magn. Reson. Chem.* **1990**, *28*, S104.
(19) Mehring, M. *Principles of High Resolution NMR in Solids*, 2nd ed.; Springer-Verlag: Berlin, 1983; Chapters 2 and 4.
(20) Muntean, J. V.; Stock, L. M.; Botto, R. E. *J. Magn. Reson.* **1988**, *76*, 540.
(21) Kenwright, A. M.; Packer, K. J.; Say, B. J. *J. Magn. Reson.* **1986**, *69*, 426.
(22) Gerstein, B. C.; Pembleton, R. G.; Wilson, R. C.; Ryan, L. M. *J. Chem. Phys.* **1977**, *66*, 361.
(23) Harris, R. K.; Jackson, P. *Magn. Reson. Chem.* ***1988***, *26*, 1003.
(24) Bronnimann, C. E.; Hawkins, B. L.; Zhang, M.; Maciel, G. E. *Anal. Chem.* **1988**, *60*, 1743.
(25) Marciel, G. E.; Bronnimann, C. E.; Hawkins, B. L. *Adv. Magn. Reson.* **1990**, *14*, 125.
(26) Burum, D. P.; Rhim, W. K. *J. Chem. Phys.* **1979**, *71B*, 944.
(27) Mansfield, P.; Ware, D. *Phys. Lett.* **1966**, *22B*, 133.
(28) Rhim, W. K.; Elleman, D. D.; Vaughan, J. *J. Chem. Phys.* **1973**, *59*, 3740.
(29) Nesbitt, G. J. Ph.D. Thesis, University of Durham, UK, 1986.
(30) Derbyshire, F.; Marzee, A.; Schulten, H. R. Wilson, M. A.; Davis, A.; Tekely, P.; Delpuech, J. J.; Jurkiewiez, A.; Bronnimann, C. E.; Wind, R. A.; Maciel, G. E.; Narayan, R.; Bartle, K.; Snape, C. E. *Fuel* **1989**, *68*, 1091.
(31) Love, G. D.; Law, R. V.; Snape, C. E. *Energy Fuels* **1993**, *7*, 639.
(32) Manatt, S. L.; Horowitz, D.; Horowitz, R.; Pinnell, R. P. *Anal. Chem.* **1980**, *52*, 1529.
(33) Ford, W. T.; Yacoub, S. A. *J. Org. Chem.* **1981**, *46*, 819.
(34) Guyot, A.; Bartholin, M. *Prog. Polym. Sci.* **1982**, *8*, 277.
(35) Mohanraj, S.; Ford, W. T. *Macromolecules* **1985**, *18*, 351.
(36) Opella, S. J.; Frey, M. H. *J. Am. Chem. Soc.* **1979**, *101*, 5854.
(37) Law, R. V. Ph.D. Thesis, University of Strathclyde, Glasgow, UK, 1994.
(38) Huxham, I. M.; Rowatt, B.; Sherrington, D. C.; Tetley, L. *Polymer* **1992**, *33*, 2768.

MA951606O